JOURNAL OF MATERIALS SCIENCE **36** (2001) 419–428

Interfacial reactions in an Al-Cu-Mg (2009)/SiC*w* composite during liquid processing

Part I *Casting*

A. UREIÑA*, P. RODRIGO, L. GIL
Dept. Ciencias Experimentales e Ingeniería. Escuela Superior de Ciencias Experimentales y Tecnología, Universidad Rey Juan Carlos, 28933 Móstoles, Madrid, Spain
E-mail: a.urena@escet.urjc.es

M. D. ESCALERA
Dept. Ciencia de los Materiales e Ingeniería Metalúrgica, Facultad de Ciencias Químicas. Universidad Complutense de Madrid, 28040 Madrid, Spain

J. L. BALDONEDO
Centro de Microscopía Electrónica "Luis Bru", Universidad Complutense de Madrid, 28040 Madrid, Spain

The interfacial reactions in an aluminium alloy composite (AA2009) reinforced with 15% volume of SiC whiskers were studied. The composite was subjected to a simulated casting process to analyse its response under different melting conditions. The different reaction mechanisms between the SiC whiskers and both the molten aluminium and their alloying elements (Cu, Mg, and Fe) are discussed. The high aspect ratio (*l*/*d*) of the reinforcement is the main microstructural factor, which controls both reactivity and wettability between the molten matrix and the SiC. Tested specimens showed very great Si-enrichment of the matrix around SiC*w* which produced an isothermal solidification and stopped the interfacial reactions. Formation of binary aluminium carbide (Al_4C_3) during the melting cycles was also detected, especially for temperatures higher than 800 °C, produced by a dissolution-precipitation mechanism. Nucleation of the Al_4C_3 crystal was favoured both on the lateral whisker surfaces and on oxide particles (Al_2O_3, MgO) present in the aluminium matrix. Transmission Electron Microscopy and Electron Diffraction (TEM-ED) studies made it possible to identify both the nature and the structure of the different interfacial products generated during casting.

1. Introduction

Aluminium matrix composites (AMC) reinforced with ceramics have some greatly improved mechanical properties, such as wear resistance, hardness, specific stiffness and strength, etc. as compared to unreinforced alloys [1]. Of particular interest among these AMCs are those reinforced with ceramic whiskers in that this is a special kind of defect-free monocrystalline reinforcement with the highest strengths. They have a smaller diameter than continuous ceramic fibres, being a discontinuous phase (with a finite *l*/*d* ratio). SiC whiskers (SiC*w*) are among those most widely used to reinforce aluminium alloys because of their advantages over other possible candidates (B, graphite, Al_2O_3, $K_2Ti_6O_{13}$ or $Al_{18}B_4O_{33}$). Their main characteristics include higher thermal conductivity, excellent corrosion resistance, great machinability and formability, and above all low fabrication costs (from rice hull pyrolysis or vapour-liquid solid synthesis from coconut hull) [2, 3].

One of the main problems presented by Al-SiC composites, and particularity whisker reinforced composites, is the difficulty of applying liquid phase procedures for their manufacture or joining. Most SiC*w*-AMCs are made by powder metallurgy (PM). Only the pressure infiltration of whisker preforms as a cast fabrication route has been applied with acceptable results [4–6]. The interfacial reactions occurring during contact between the molten matrix and the reinforcement is one of the problems that limits the processability of these composites. These problems not only affect the interface strength but also other aspects relating to the mechanical behaviour of the matrix, such as age-hardening mechanisms, or wettability between the two components.

The reaction between molten aluminium and SiC in the temperature range 650–900 °C has been studied

* Author to whom all correspondence should be addressed.

by many authors [7–10]. However, most have worked with bulk or particulate SiC. These studies have shown that the interface reaction is produced by a dissolution-renucleation process. However, there have been only a few studies on interfacial reactivity with SiC whiskers under conventional remelting test [11], and none on arc welding, which will be also analysed in a second part of this work [12]. Under these special conditions, the reaction mechanisms have not been established, and it would be of interest to determine their influence on the composite microstructure.

This paper describes a detailed investigation of the reaction mechanisms between SiC whiskers and an Al-Cu-Mg (AA2009) alloy under conventional casting conditions. Of particular interest were the effects of the alloying elements, the melting conditions (time and temperature) and the nature of the SiC whiskers on the interfacial reactions. For this study, light (LM), scanning (SEM) and transmission electron microscopy (TEM) were used along with electron diffraction (ED) and other structural and microanalytical techniques such as X-ray diffraction (XRD) and energy dispersive X-ray spectrometry (EDS), whereby the interface products were identified. In the second part of the paper [12], the influence of more energetic fusion conditions, such as those reached during arc welding of composite materials, is analysed by comparing the differences in interfacial reactivity between cast and welded composites.

2. Experimental procedure

2.1. Parent composite

The composite material used for the present investigation was an aluminium alloy AA2009, whose nominal composition appears in Table I, reinforced with a 15 volume percentage of SiC whiskers. This material was manufactured by Advanced Composites Materials Corporation (ACMC) by a PM route and was received in a 20 mm thick extruded plate with a T83 temper. This material as received is characterised by high stiffness and strength combined with moderate damage tolerance as compared to conventional unreinforced aluminium alloys. Table II compares the mechanical properties of the parent composite (2009/SiC/15*w*) with those of other unreinforced aluminium alloys.

TABLE I Nominal composition of the matrix alloy A2009 (weight %)

Cu	Mg	Zn	Si	Fe	O	Others (each one)	Others (all)	Al
3,2-4,4	1,0-1,6	0,10	0,25	0,07	0,6	0,05	0,15	Bal.

TABLE II Mechanical properties of the 2009/SiC/15w composite compared with other commercial aluminium alloys (T6 condition)

Material	Tensile Strength (MPa)	Yield Strength (MPa)	Elastic Modulus (GPa)	Elongation (%)
AA2009/SiC/15w	642	448.5	106.3	3
AA7075	573	504	72	11
AA2024	476	393	73,1	10

TABLE III Vacuum melting conditions applied to the parent composite

Temperature (°C)	750	800	850	850	850	900
time (min)	60	15	30	15	60	15

2.2. Reactivity tests by controlled melting (casting) and characterisation studies

A vacuum fusion test that simulated casting procedures was used to study the reactivity between SiC whiskers and AA2009 matrix alloy in molten phase. One piece of the parent composite was melted in an alumina crucible using a vacuum furnace (10^{-4} Pa); fusion conditions are shown in Table III.

Both parent and tested materials were characterised by light microscopy (LM), SEM (JEOL models 35C and 6400) and TEM (JEOL model 2000 FX). The interface microstructure was examined using bright field (BF) and dark field (DF) images, electron diffraction (ED) and energy dispersive X-ray spectroscopy (EDS). Prior to these studies, bulk structural changes in the composite under the different testing conditions were monitored by X-ray diffraction (XRD) using a Cu anticathode (Cu $K_\alpha = 1.5405$ Å).

The TEM thin foils were prepared by ion milling at 5 kV and 1 mA, keeping the temperature at 20 °C and using an Ar^+ beam with an incidence angle of 15°. Specimens had first been mechanically polished and dimpled. All the polishing and grinding operations were performed using ethylene glycol as lubricant to avoid water degradation of the reaction products (especially of the formed Al_4C_3).

3. Results

3.1. Microstructure of the AA2009/SiC/15*w* as-received composite

Fig. 1 is a 3-D SEM micrographic composition showing the distribution of SiC whiskers inside the aluminium matrix, with the characteristic preferential orientation produced by the extrusion process used to manufacture the composite plate from the PM pieces. Whisker lengths ranged from 5 to 20 μm, with an average diameter of 0.5 μm. Faults in the distribution of whiskers are appreciable (banding and clustering) in Fig. 2a and b. The composite matrix had an elongated grain structure with length in the range of 15–20 μm. However, recrystallisation was favoured in rich-reinforcement bands where an equiaxial microstructure had developed with grain sizes smaller than 5 μm.

TEM-ED studies showed that whiskers used as reinforcement were hexagonal (α-SiC-6H), characterised by flat ends forming a sharp 90° corner around the end section and by the presence of an internal banded structure formed by microtwins along the {0001} planes. Both kinds of microstructural characteristic can be seen in Fig. 3, which also shows the ED patterns obtained from two different zone axes.

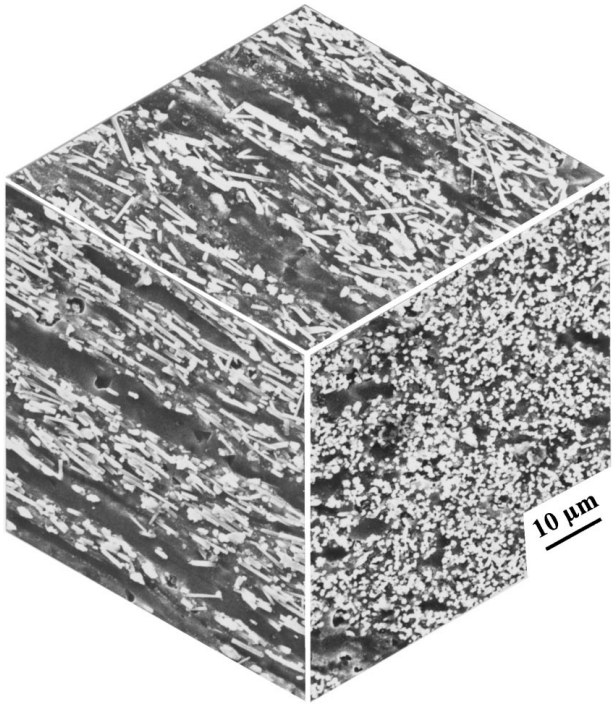

Figure 1 Tree dimensional SEM microstructure of the parent composite plate.

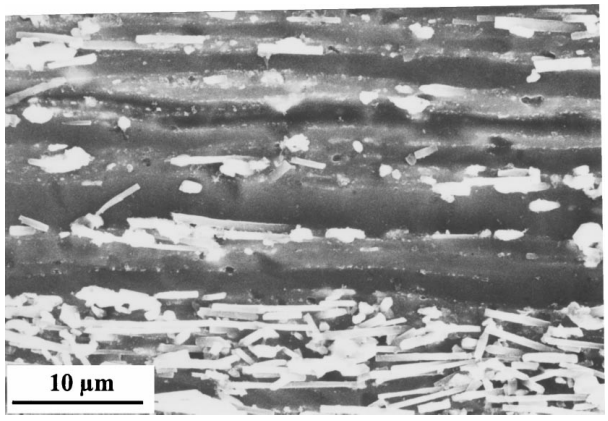

(a)

(b)

Figure 2 Faults of whisker distribution in the composite. a) banding, b) clustering.

Fig. 4 shows a detail of the whisker-matrix interface in which the SiC reinforcement has not been attacked by the matrix. In general, the interface was free of reaction products and only two significant details were

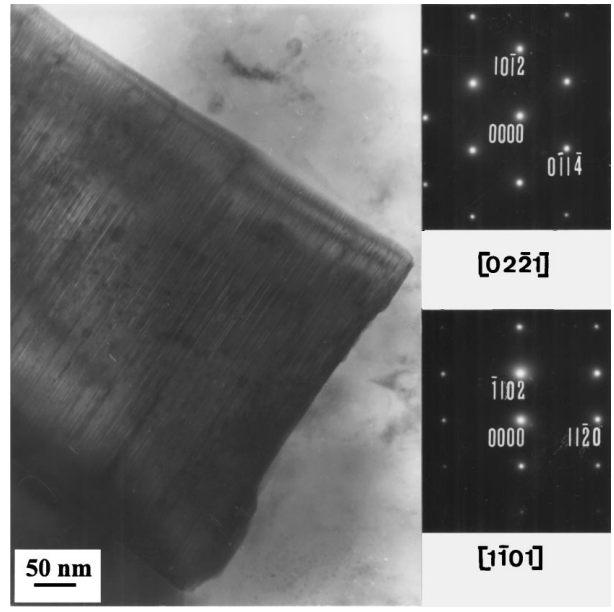

Figure 3 TEM detail of a α-whisker edge showing the ED patterns of the [02$\bar{2}$1] and [1$\bar{1}$01] zone axis.

Figure 4 TEM detail of recrystalization in a whisker corner (marked with arrow).

observed: 1) the preferential nucleation of new recrystallized aluminium grains, associated with the whisker corners where intense plastic straining in the nearby matrix is generated; and 2) the presence of oxide inclusions, mainly Al_2O_3 crystals, associated with Mg (Fig. 5a and b). These oxide phases originate in the oxide layer which surrounds the aluminium powder used in the composite manufacture, which usually reacts with Mg also present in the 2009 alloy.

Matrix grains showed preferential precipitation of lath-shape phases identified as the semi-coherent S' (orthorhombic Al_2CuMg) phase, which is one of those responsible for age hardening of the matrix. However, most of the Cu was associated with the equilibrium Al_2Cu precipitates (θ phase), and a semi-coherent θ' phase was not found. Some of these equilibrium precipitates were associated with whiskers.

3.2. Microstructure of the vacuum melted composite

Before their microstructure was studied, the vacuum melted composites were characterised by XRD,

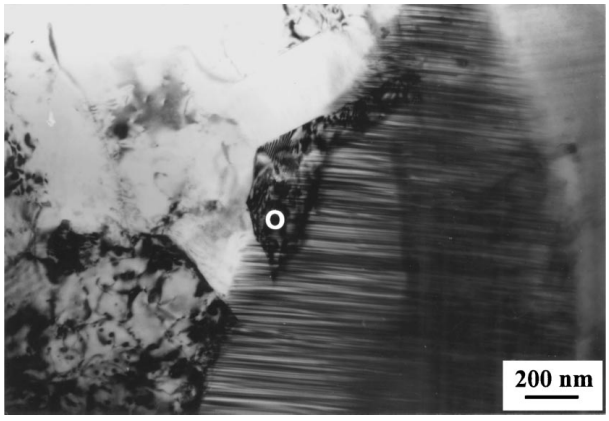

(a)

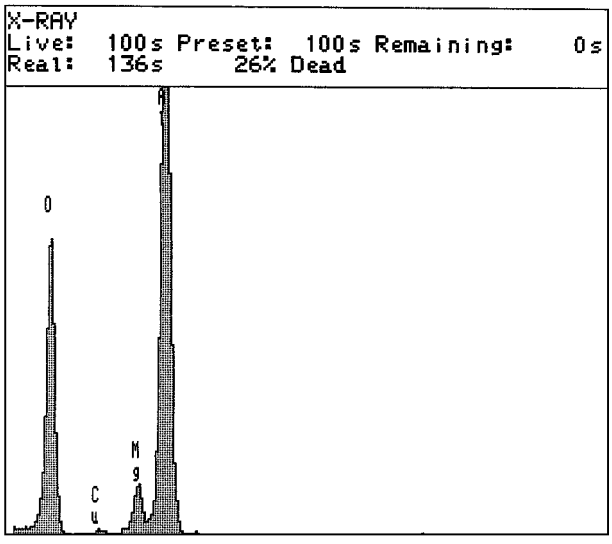

(b)

Figure 5 a) Inclusion oxide in the matrix/whisker interface. b) EDX microanalysis of the oxide (marked with O).

comparing the results for each melting condition with those of the as-received parent composite. Fig. 6 shows the X-ray diffraction patterns of the AA2009/SiC15*w* composite, before melting treatment (a) and after 60 min at 750 and 850 °C respectively (b and c). The main observed changes are related to Si-enrichment of the materials, which is manifested firstly by the formation of Si-rich intermetallic phases (Cu_4Si), and when these alloying elements are consumed, by formation of a high proportion of elementary Si.

Another noticeable change, which occurred even at the low temperature (750 °C), was the formation of Al_4C_3, with progressive consumption of the SiC whiskers. However, although higher temperatures favour the formation of aluminium carbide, this never occurred fully in the experimental conditions. Apart from this, the formation of Al_2MgO_4 spinel seems to be favoured by matrix melting.

LM and SEM observations of melted specimens showed two main changes in the composite microstructure: 1) modification in the distribution of SiC whiskers and 2) formation of new phases due to reaction between the reinforcement and the matrix elements. In general, for melting temperatures down to 800 °C, there were no noticeable changes in whisker arrangement; the most significant change was the formation of porosity (micropipes) originated by contraction during matrix solidification (Fig. 7a). The inner surfaces of these voids were covered by SiC whiskers (Fig. 7b), which had been subjected to the agitation of the molten pool, but they retained there original lengths.

The increase of melting temperature favoured reinforcement redistribution. At 800 °C, the solidification front drove whiskers to accumulate inside the aluminium intercellular spaces. Under these conditions, the microstructure of the composite was reorganised with zones containing high proportions of SiC whiskers where the first sign of interfacial reaction appeared. Other reinforcement-free areas were formed by large aluminium grains with needled intermetallic phases that precipitated during cooling (Fig. 8). These phases were constituted mainly by Si and other equilibrium intermetallic phases of the AA2009.

The main effect of the interface reaction in the zones of whisker accumulation was the formation of Si lakes, which contained partially-dissolved SiC*w*. These Si lakes became more extensive as the melting temperature increased. At 900 °C, (see Fig. 9) a large area of the matrix was covered by these Si aggregates, and other undissolved whiskers were detected inside them.

TEM-ED studies confirmed that these reaction products were mainly composed of elementary Si. Fig. 10 shows a detail of a SiC whisker surrounded by Si as confirmed ED. A crack inside the Si phase is appreciable. Si enrichment of the aluminium matrix not only produced the formation of those previous continuous aggregates, but also favoured the formation of other minority intermetallic phases such as $Al_{1.9}CuMg_{4.1}Si_{3.3}$, whose TEM image, EDS microanalysis and ED patterns are shown in Fig. 11.

The other main product formed by the reaction between SiC and molten Al is Al_4C_3. Its presence was detected by the XRD study, even in specimens melted at 750 °C, but was more difficult to confirm by SEM observation. These examinations showed that Al_4C_3 usually appeared associated with lateral SiC*w* surfaces from which they had nucleated and grown, but it mainly occurred in whiskers which were not surrounded by Si lakes. Fig. 12a shows several of these Al_4C_3 crystals growing on a SiC whisker. The deep metallographic etching of the aluminium matrix has developed their structures, which consist of hexagonal crystals that grow parallel to their basal planes. EDS confirmed that the composition, although associated with Al and C, always appeared O due to the hydrolysis normally undergone by Al_4C_3 (Fig. 12b). TEM-ED studies showed the hexagonal cross-section of these crystals, which usually nucleated on the whisker lateral surfaces (Fig. 13).

TEM micrographs showed that Al_4C_3 crystals also used other solid interfaces present in the molten aluminium (i.e. oxide particles) to nucleate. Fig. 14 shows the formation of one of these crystals with a high proportion of MgO dispersoids inside it. C-enrichment of the molten aluminium caused by progressive dissolution of the SiC, combined with the low solubility of C in Al (15 ppm at 1000 K), produced rapid precipitation as Al_4C_3, using the solid-liquid interfaces for heterogeneous nucleation.

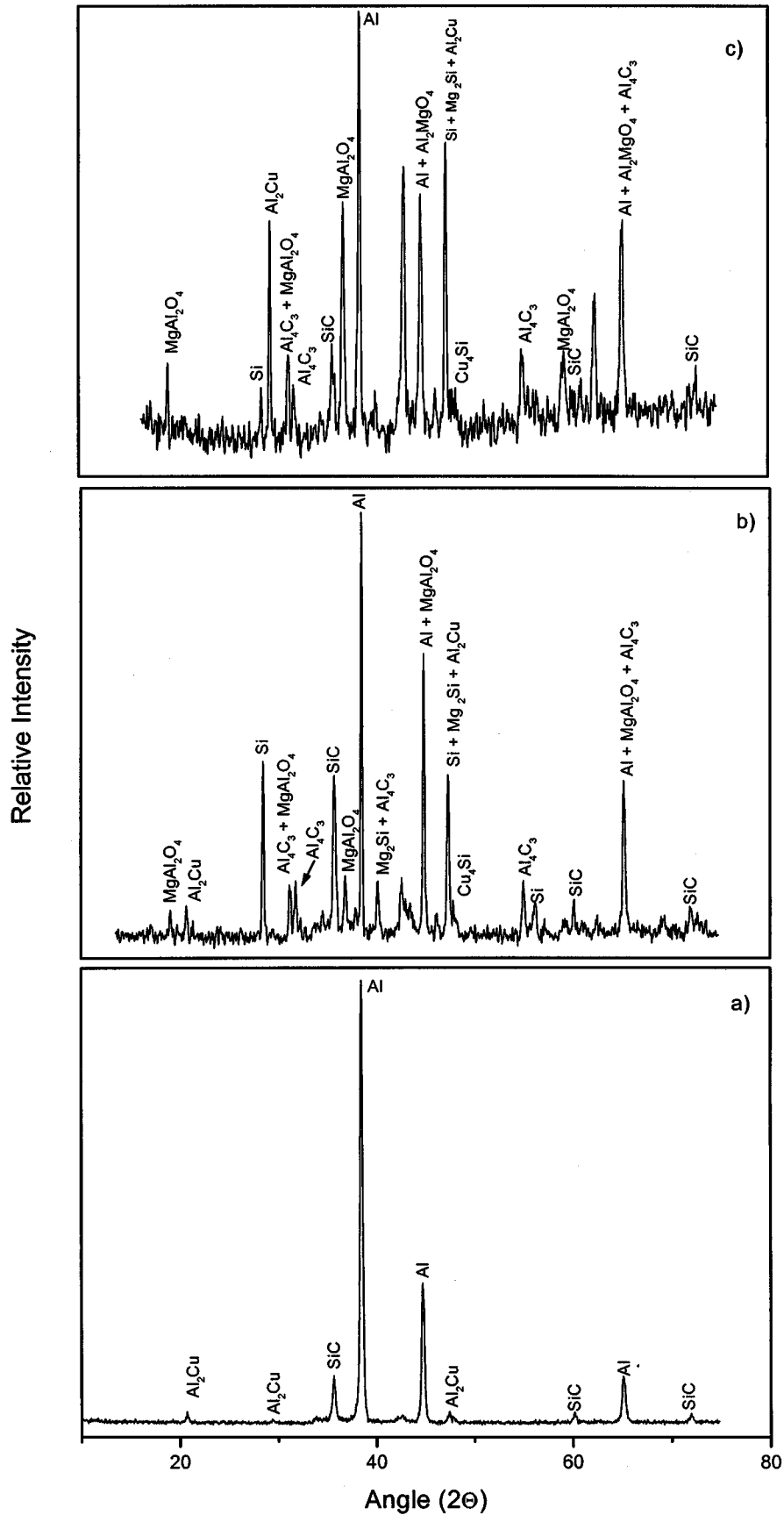

Figure 6 XRD patterns of the parent composite: a) as-received condition, b) melted at 750 °C for 60 min, c) melted at 850 °C for 60 min.

The presence of ideomorphic crystals of the Al_2MgO_4 spinel was determined by TEM-ED studies. Fig. 15 shows a TEM micrograph where there are two of these crystals, and also their EDS microanalysis and ED pattern. The formation of these aggregates is not necessarily related to the casting procedure, although XRD studies showed that their proportion increased during the fusion tests.

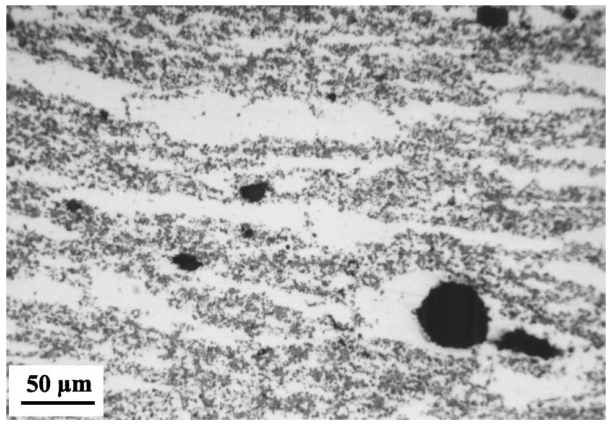

(a)

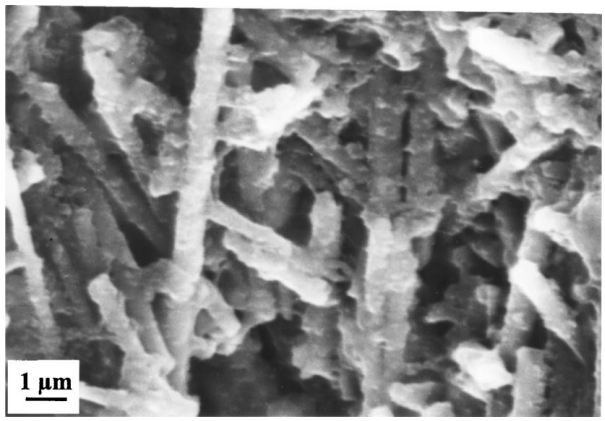

(b)

Figure 7 a) Microporosity formed during composite solidification (melted at 800 °C). b) SEM detail of the SiC whiskers inside a solidification void.

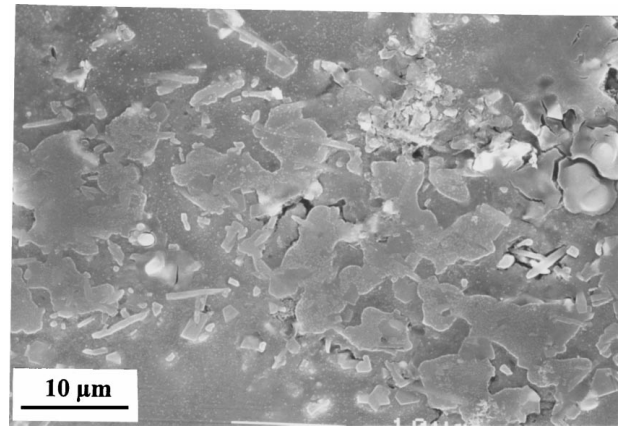

(a)

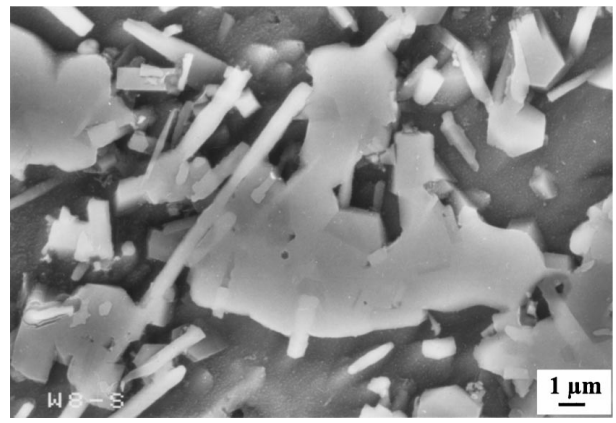

(b)

Figure 9 a) Si aggregates formed by Si-enrichment of the matrix after melting at 900 °C. b) Backscattered image of the free Si crystals surrounding SiC whiskers.

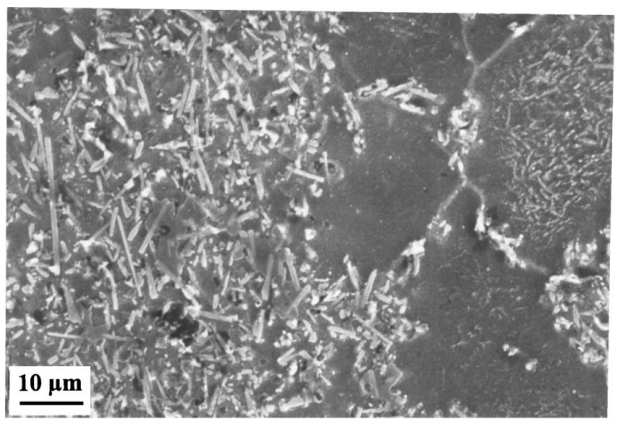

Figure 8 Redistribution of reinforcement after solidification in a composite specimen melted at 800 °C.

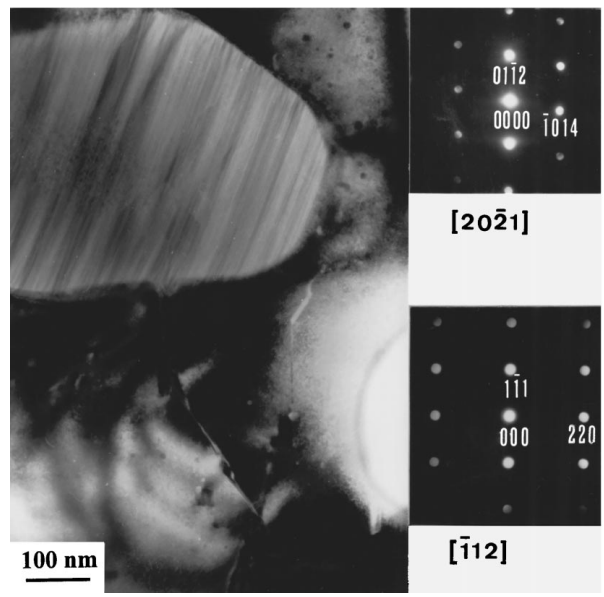

Figure 10 TEM image of a SiC*w* cross section inside a Si lake including the ED patters of α-SiC whisker [20$\bar{2}$1] and Si [$\bar{1}$12].

4. Discussion

The microscopic and microanalytical studies described in the previous section raise the following points regarding the casting behaviour of SiC whisker reinforced aluminium composites.

4.1. Influence of reinforcement morphology

The above results suggest that not only the chemical composition of the ceramic compound used as reinforcement (SiC), but also the shape of the whiskers, are two of the main factors determining the nature and extent of the interface reactions with the molten aluminium alloy. The present authors established the microstructural characteristics of interface reactions in SiC particulate composites with a similar degree of reinforcement (13% vol.) [13], and they found important differences from the behaviour of

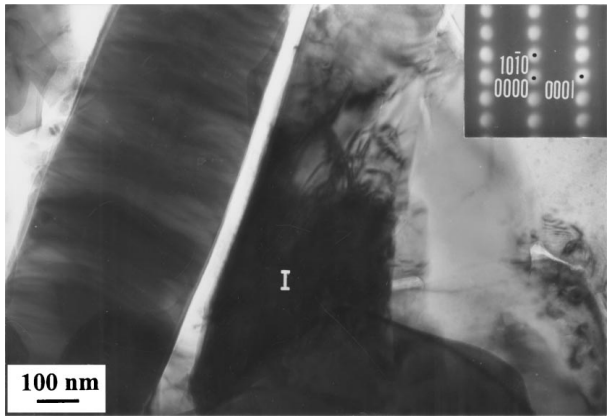

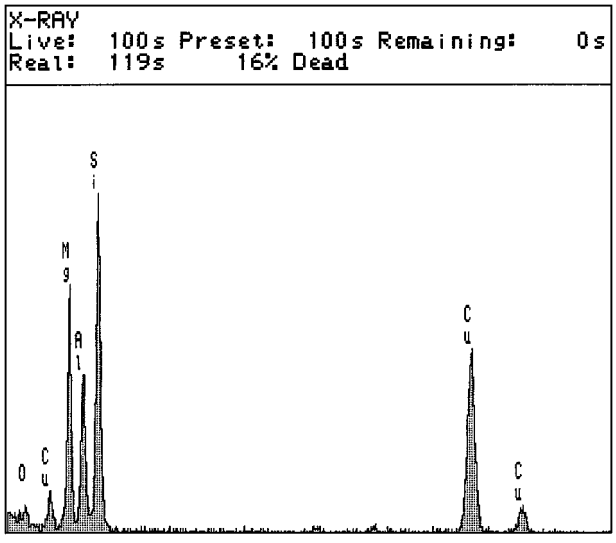

Figure 11 TEM image of an intermetallic compound identified as $Al_{1.9}CuMg_{4.1}Si_{3.3}$, marked as I, including its ED pattern and EDX microanalysis.

(a)

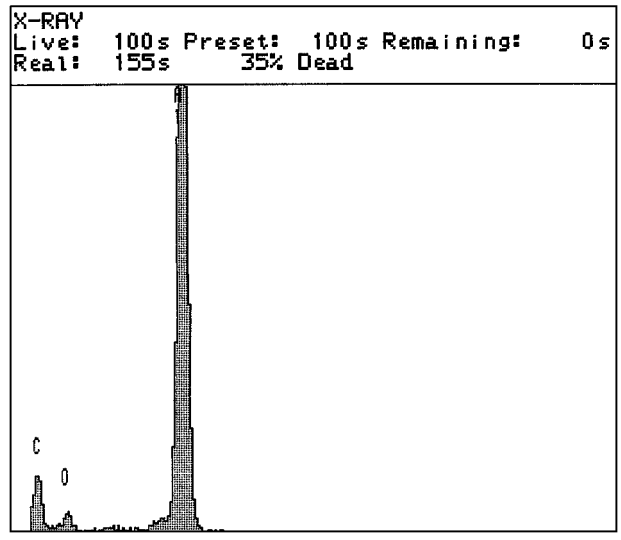

(b)

Figure 12 a) Al_4C_3 crystals growing on the SiC whisker surface. b) EDX microanalysis of the reaction product, showing the presence of O due to its partial hydrolysis.

the whisker reinforced material under similar casting conditions.

These differences are mainly caused by two different reason related with the whiskers structure and morphologies: 1) the higher aspect ratio (l/d) of the whiskers in relation with particles which produces an increase in the proportion of SiC/Al interface for the whisker-reinforced composites; and 2) the single crystalline structure of whiskers which condition their behaviour in molten aluminium.

Increasing the metal/ceramic interface area in composite reinforced ceramic whiskers aggravates the wettability problems. The increase in ceramic surfaces to be wetted and the higher viscosity of the melted phase due to the high proportion of solid ceramic component are both factors that limit this necessary wetting phenomenon. When aluminium alloy begins to solidify, the solid whiskers are pushed by the solidification front. The pushing effect is caused by a disjointing force exerted on the whisker by the advancing front, due to the raising of the total interfacial energy by formation of a solid/liquid interface. This originates a redistribution of the SiC whisker inside the solidified matrix. In those zones where the whiskers have accumulated, contraction during aluminium solidification produces the formation of inner pipes (pores) whose surfaces are covered by virtually unaltered whiskers. This explains why the composite specimens melted at up to 900°C did not lose their original shapes and the matrix melting only produced a light swelling through the increase of internal porosity. This effect could limit the time and area of effective contact between both reactive phases (molten aluminium and solid SiC), and therefore the proportion of solid Al_4C_3 generated by means of the reaction:

$$Al(l) + SiC(s) \rightarrow Al_4C_3(s) + Si_{[Al]} \qquad (1)$$

The other effect is the special structure of whiskers which are α-hexagonal SiC single crystals with a polar structure. This kind of crystalline structure is very different to the policrystalline one of SiC particles, being also responsible of the different degree of reactivity which can be noticed by the higher proportion of the Si-rich aggregates formed and the lower interface generation of Al_4C_3, in relation with particulated composites. Present authors have carried out a deep study of the interface reactivity in AA2014/SiCp composites after casting and welding [13]. This study showed that low-energy melting processes (i.e. casting) of these materials favour consumption of the reinforcement by interface reaction and formation of hexagonal Al_4C_3 crystal, which were nucleated preferentially in certain

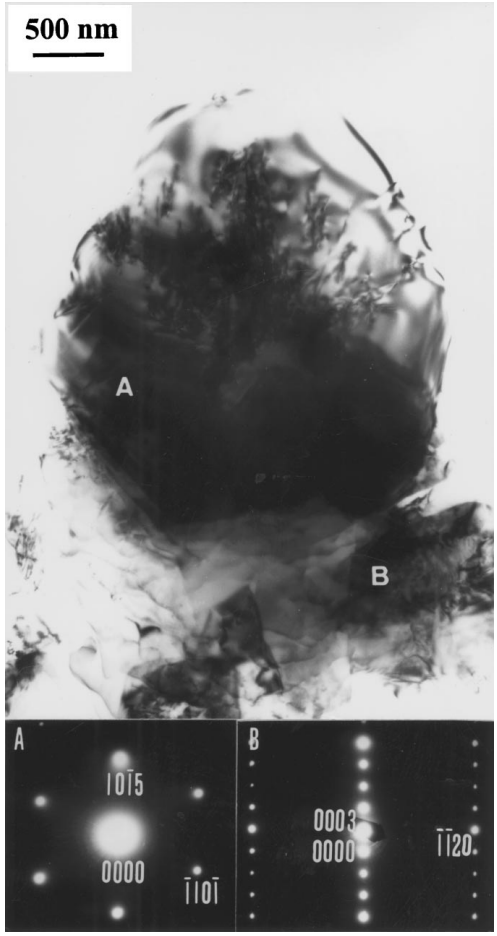

Figure 13 TEM images of two Al_4C_3 crystals (marked with A and B) with different orientation. ED patterns of both crystals.

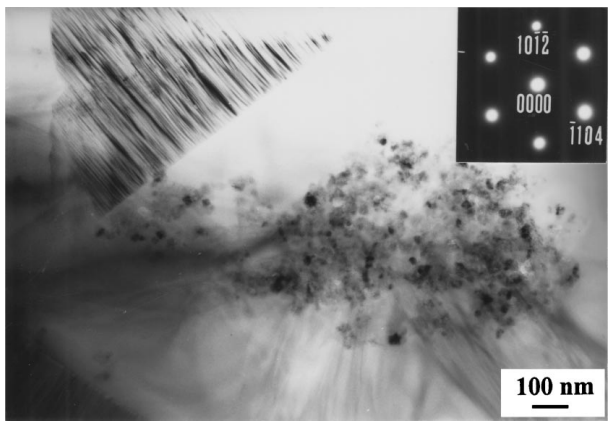

Figure 14 Oxide inclusion (MgO) inside Al_4C_3 crystal nucleated in the matrix. ED pattern of the aluminium carbide.

planes of the SiC, accelerating SiC dissolution in uncovered areas. Next points discuss both the formation of continuous Si aggregates and the special characteristics of the Al_4C_3 generation, which is the main difference observed in casting of Al/SiCw composites.

4.2. Formation of Si-rich phases

When interfacial reaction (1) starts, the generated Si interacts with alloying elements of the matrix, such as Cu, Mg or Fe, to form the intermetallic compounds which were detected and identified by SEM and TEM-ED

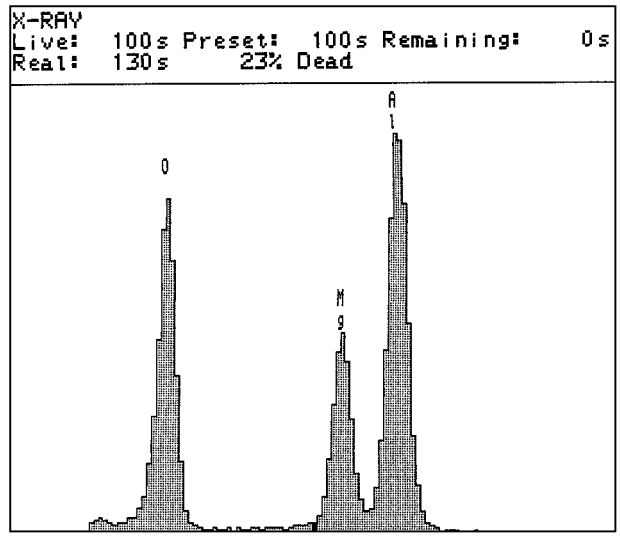

Figure 15 TEM image of a crystal of Al_2MgO_4 spinel detected in the composite matrix after melting treatment. ED pattern and EDX microanalysis of the spinel.

(Cu_4Si, $Al_{1.9}CuMg_{4.1}Si_{3.3}$, AlSiFe). This would decrease the activity of free-Si in molten aluminium, which in turn would thermodynamically favour the interfacial reaction. This kind of behaviour had been also described by present authors for Al/SiCp composites [13], being very similar for Al/SiCw ones.

However, when those alloying elements are drained in the molten matrix which surrounds the whiskers, the proportion of free-Si in those zones would increase as long as the whiskers were dissolved. The very high viscosity of the liquid phase and the high proportion of solid/liquid interface hinder the diffusion and homogenisation of the Si into the molten aluminium. Under these conditions, Si concentration around whisker accumulation zones could reach levels high enough to favour the formation of the elemental Si aggregates by an isothermal solidification mechanism. The formation of these Si lakes produces the separation of both reactive substances (SiC*w* and molten Al), which is why dissolution of the SiC is rarely completed.

4.3. Formation of aluminium carbide

Formation of Al_4C_3 was only observed by SEM-TEM in specimens melted at temperatures higher than 800 °C. Nevertheless, XRD also detected the presence of this compound in specimens melted at 750 °C.

However, reaction (1) has a slow kinetic and the formation of Al_4C_3 is not favoured at low temperatures.

On the other hand, when the C concentration exceeds its solubility limit in molten Al, Al_4C_3 formation is produced by prior dissolution of the SiC whiskers in the molten aluminium followed by Al_4C_3 precipitation. This favours heterogeneous nucleation of the Al_4C_3 crystals. Two preferential zones for the nucleation have been identified: (i) on the SiC whisker lateral surfaces, and (ii) on stable oxide particles present in the metallic matrix.

The microstructural study using SEM and TEM showed the existence of platelet Al_4C_3 crystals with hexagonal morphologies, preferentially nucleated at certain places on the whisker lateral surfaces and growing towards the metallic matrix. These observations proved the existence of a mechanism of *dissolution-precipitation* for formation of Al_4C_3. However, the heterogeneous nucleation on the same whisker surface in dissolution, which is the main mechanism identified for other aluminium matrix composites discontinuously reinforced with SiC (i.e. particulate ones) [13], is less favourable for monocrystalline reinforcements. The reason for this behaviour is related, as previously has been pointed, to the crystalline structure of the SiC whiskers.

It has been observed from TEM images that there are two kinds of SiC/Al interfaces after casting tests: ones that have practically not reacted and others with irregular morphology, which show whisker consumption by preferential dissolution. From studies carried out by Viala *et al*. [9, 10] it can be deduced that those crystalline planes of the SiC composed only of Si or of both Si and C atoms have a higher reactivity than atomic planes composed only of C. For this reason, platelet Al_4C_3 crystals appear mainly on the lateral surface of α-SiC (6H) whisker $\{11\bar{2}0\}$ planes, which contains both Si and C atoms. On the other hand, the edges of the whisker are the basal {0001} planes which, due to the polar structure of α-hexagonal SiC single crystals, may be formed by Si atoms (0001) or "Si faces" or by C atoms $(000\bar{1})$ or "carbon faces". In the first case, dissolution is favoured (the C faces is dissolved 6 or 7 times slower than Si ones), which explain also the higher enrichment of Si in this kind of composites, and in fact some whiskers partially dissolved at the edges were observed. But if the whisker edge is a plane of C atoms, the rate of dissolution in molten aluminium will be lower. Some authors have also established that the Al_4C_3 crystallites usually nucleate with their *c*-axis oriented in a direction parallel to the *c*-axis of the SiC crystal, which means that the principal places for formation of Al_4C_3 would be the (0001) Si-planes. However, the higher Si-enrichment and the lower concentration of C in the molten matrix around these zones limit the Al_4C_3 formation on the whiskers edges.

The other mechanism for nucleation of Al_4C_3 was detected in crystals formed inside the matrix alloy, and not directly on the SiC whiskers. In this case, the existence of other solid aggregates, which are stable in molten aluminium at casting temperature (i.e. aluminium or magnesium oxides), are used for heterogeneous nucleation, when C concentration in molten aluminium is higher than its solubility limits.

These oxide phases (MgO, Al_2O_3) do not form during casting treatment but come from the matrix powders used during composite fabrication by a PM route. An increase of X-ray signal intensity with casting temperature was measured only for the case of the Al-Mg spinel ($MgAl_2O_4$). For this reason, its formation could have been favoured by the reaction of Mg dissolved in molten Al, with the aluminium oxides that had been detected in the parent composite. The possible reaction for formation of the spinel would be:

$$3Mg + Al_2O_3 \rightarrow 3MgO + 2Al \quad (2)$$

$$MgO + Al_2O_3 \rightarrow MgAl_2O_4 \quad (3)$$

$$3Mg + 4Al_2O_3 \rightarrow 3MgAl_2O_4 + 2Al \quad (4)$$

These reactions would produce a depletion of Mg in the aluminium alloy, which would explain why a lower proportion of Mg-rich intermetallic compounds was detected after casting tests.

5. Conclusions

1. The monocrystalline structure of the SiC whiskers (α-SiC 6H) conditions the dissolution mechanisms in molten aluminium, and is one of the controls factors which determines, jointly the local accumulation of SiC whiskers, the high Si enrichments during remelting of Al-SiCw composites and the formation of continuous Si aggregates, by isothermal solidification, around partially dissolved whiskers.

2. Other factor which determines the melting behaviour of an aluminium alloy reinforced with SiC whiskers as compared with other discontinuously reinforced composites (i.e. particulate ones) is the greater aspect ratio (l/d) of this kind of reinforcements. In this case, the increase of the metal-ceramic interface area produces wettability problems that cause discontinuities (porosity, reinforcement clustering, etc.) in fabricated products.

3. The formation of Al_4C_3 crystal occurs by a dissolution-precipitation mechanism, especially at temperatures higher than 800 °C. The nucleation of these aggregates mainly occurs on the lateral SiC whisker surfaces (formed by atomic planes which have both Si and C atoms) or on other stable oxide compounds (Al_2O_3, MgO) present in the matrix alloy.

4. It was observed that the melting of the composite favoured the formation of Al-Mg spinel ($MgAl_2O_4$) which produced a depletion of Mg in the solidified matrix.

Acknowledgements

Authors wish to thank the *Comisión Interministerial de Ciencia y Tecnología (CICYT)* for its financial support in the preparation of this study (Project MAT97/0719).

References

1. D. J. LLOYD, *Int. Mat. Rev.* **39** (1994) 1.
2. S. V. NAIR, J. K. TIEN and R. C. BATES, *Int. Met. Rev.* **30** (1985) 275.
3. A. V. SELVEM, N. G. NAIR and P. SING, *J. Mater. Sci.* **17** (1998) 57.
4. W. J. PARK and N. J. KIM, *Script. Mat.* **36** (1997) 1045.
5. D. Z. YANG, S. L. DONG, J. F. MAO and Y. X. CUI, *Key Eng. Mat.* **104–107** (1995) 627.
6. L. GENG, K. WU and G. K. YAO, *Mater. Charact.* **34** (1995) 227.
7. D. S. SHIN, J. C. LEE, E. P. YOOH and H. I. LEE, *Mat. Res. Bull.* **32** (1997) 1155.
8. K. B. LEE and H. KWON, *Script. Mat.* **36** (1997) 847.
9. J. C. VIALA, P. FORTIER and J. BOUIX, *J. Mater. Sci.* **25** (1990) 1842.
10. J. C. VIALA, F. BOSSELET, V. LAURENT and Y. LEPETITCORPS, *ibid.* **28** (1993) 5301.
11. S. W. LAI and D. D. L. CHUNG, *J. Mater. Chem.* **6** (1996) 469.
12. A. UREÑA, P. RODRIGO, L. GIL, M. D. ESCALERA and J. L. BALDONEDO, *J. Mater. Sci.* (2000), in press.
13. A. UREÑA, J. M. GÓMEZ DE SALAZAR, L. GIL, M. D. ESCALERA and J. L. BALDONEDO, *J. Microscopy* **196** (2) (1999) 124.

Received 25 October 1999
and accepted 6 July 2000